Int. J. Metrol. Qual. Eng. **15**, 9 (2024)

https://doi.org/10.1051/ijmqe/2024007

International Journal of Metrology and Quality Engineering

Available online at:
www.metrology-journal.org

RESEARCH ARTICLE OPEN ACCESS

Investigation of the impact of cycloidal gear pin tooth wear on transmission error in precision planetary cycloidal reducers

Hang Xu[1,2,3,*], Chenzhou Wei[1,2], Wei Gui[1,2], Shufeng Yang[1,2], Yuanchun He[3], Guiping Xie[3], and Yaoting Wu[3]

[1] Zhongyuan University of Technology, 41 Zhongyuan Middle Road, Zhengzhou city, Henan Province, China
[2] Key Laboratory of Optical Sensing and Testing Technology for Mechanical Industry, 41 Zhongyuan Middle Road, Zhengzhou city, Henan Province, China
[3] Zhejiang Xiasha Precision Manufacturing Co., Ltd., 389 Rongji Road, Ningbo City, Zhejiang Province, China

Received: 31 October 2023 / Accepted: 16 April 2024

Abstract. In light of the alteration pattern of transmission error following wear of a cycloid gear and needle tooth, this study employs the precision planetary cycloidal 80E reducer as an example. Theoretical deduction and simulation analysis of the change in transmission error were conducted, relying on the Archard wear model and an error model. Utilizing the principles of Archard wear theory and error theory, a functional relationship between wear duration and transmission error is deduced. Subsequently, a dynamic simulation of the 3D model is executed using ADAMS software, and the simulation results are processed with MATLAB software. A comparative and analytical examination is conducted between the theoretical curve and the simulation curve of transmission error to explore the influence of the cycloid gear and needle tooth wear on transmission error. Finally, the precision of the simulation results is further confirmed through experimental validation. The findings revealed that the transmission error curve gradually increased during the initial wear of the cycloid gear and the needle tooth, with the rate of increase increasing proportionally with wear duration. By comparing the theoretical calculations, simulation outcomes, and experimental results, the validity and accuracy of the transmission error calculations grounded in Archard wear theory and error theory are confirmed. This research provides a theoretical basis for accurately predicting the survival of precision planetary cycloidal reducers throughout the lifespan.

Keywords: Precise planetary cycloidal reducer / transmission error / wear amount / Archard wear mode

1 Introduction

Precision planetary cycloid reducers offer several advantages, including high precision, efficiency, stiffness, substantial transmission ratios, and compact size. These attributes make them widely employed in industrial robotics and related domains. Among the critical components of precision planetary cycloid reducers, the cycloid gear assumes a pivotal role. The profile shape, machining errors, and wear of this gear profoundly impact the transmission accuracy of the reducer [1]. As the cycloid gear wears over time, its precision decreases. Hence, it is imperative to investigate the repercussions of cycloid gear wear on the transmission error of the reducer. Traditional experimental methods are both expensive and time-consuming, rendering them unsuitable for rapidly assessing gear wear conditions.

With the rapid advancement of virtual simulation technology, scholars both domestically and internationally have integrated gear wear theory with virtual simulation techniques, enabling the simulation analysis of gear wear through modeling. For instance, Pan Baisong et al. [2] established a harmonic gear transmission error analysis model considering wear and deformation and completed an accuracy reliability analysis combined with actual working conditions; however, the model ignored the variation in accuracy over time during wear. Zeng Ke [3] conducted contact strength and wear calculations, focusing on the accelerated wear state of worm gear reducers, based on Hertz, Archard, and elastic flow models. However, the motor state controlled by an algorithm cannot guarantee the accuracy and stability of the test system. Li Junyang et al. [4] incorporated the load of micro-convex bearings into an accelerated life model of adhesive wear and conducted accelerated life tests and statistical analyses of the data distribution under different working conditions; however, the conditional factors of the test were relatively simple. Wang Lei [5] investigated the wear mechanism of

* Corresponding author: xuhangzzti@126.com

harmonic reducers under lubrication conditions and formulated transmission error and reliability analysis models for reducing wear. However, considering only the failure mode of the transmission accuracy, no further study of the reliability of the different failure modes has been performed. Lin Zongkai [6] studied the Gaussian process regression model and used a small number of wear samples to predict the wear amount of gears, avoiding a large number of wear tests and shortening the analysis period. Wang Shuren et al. [7] conducted wear tests on involute straight cylindrical gears by employing a high-precision three-coordinate measuring instrument to assess gear tooth profiles before and after wear. The wear test procedure of the gear was determined, providing direction for subsequent test optimization. Song Wencheng [8] analyzed wear patterns in high-precision synchronous transmission involving helical gears and built a wear calculation model using the Hertzian contact pressure formula to provide theoretical support for subsequent wear simulation. Cao Jinran et al. [9] introduced an online support vector machine (SVR) prediction algorithm utilizing a combined kernel function to predict wear failures in crane gearboxes and used the algorithm to dynamically adjust the parameters of the prediction model to improve the prediction accuracy.

The Archard wear model proves to be highly adaptable, with different formulations applicable to various wear structures. In accordance with wear theory, the dimensionality of cycloid wheel teeth is reduced, effectively transforming a complex three-dimensional problem into a solvable two-dimensional problem concerning tooth mesh contact and wear. Wear-induced alterations in motion and force in the cycloid wheel occur at discrete points, which exacerbates the broader tooth wear problem. The contact pressure differs across the contact points on the cycloid wheel's tooth profile, rendering the Archard wear model a suitable choice for calculating tooth wear.

This study relies on the Archard wear model and an error model as the theoretical foundation for computing the wear experienced by cycloidal gears and pin teeth. By establishing a 3D model post-wear, the dynamics are simulated and analyzed with MATLAB software to compute the simulation results. These results yield the variation curve of the transmission error in the precision planetary cycloid reducer over the wear duration of the cycloid gear and needle teeth, allowing for an exploration of the impact of wear time on the transmission error. By comparing the simulation results with the theoretical calculations, the error range is obtained, after which the life of the cycloidal reducer is predicted. Compared with the existing theoretical calculation technology, long-term life testing of the reducer can be avoided, and the transmission error performance of the reducer can be improved in the design stage.

2 Transmission error calculation considering wear

2.1 Wear calculation model

During the operation of the reducer, the wear on the profile of the cycloid gear teeth results from a combination of wear forms, including galling, abrasive wear, and corrosive wear.

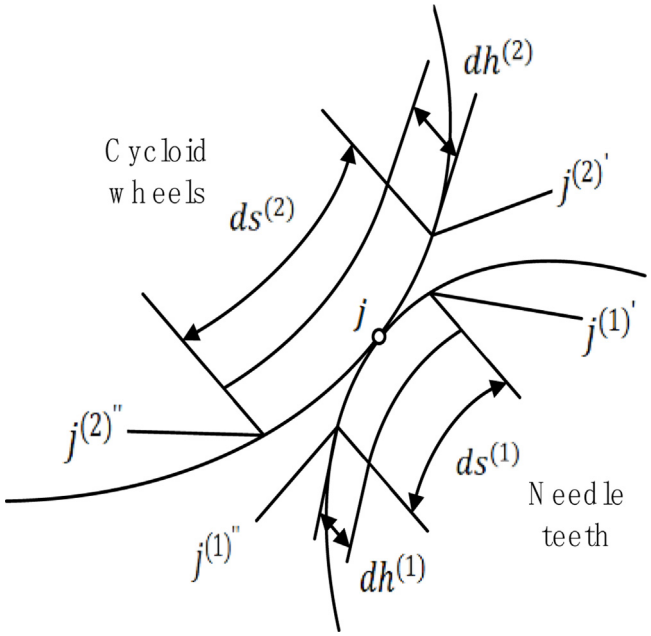

Fig. 1. Schematic illustration of cycloid gear engagement with needle teeth.

Various wear models exist, and this paper employs the Archard model to quantify wear on the trimmed cycloid gear profile [10].

As depicted in Figure 1, when the cycloid gear comes into contact with the needle tooth, the needle tooth at $j^{(1)}$ engages with the cycloid gear at $j^{(2)}$. After a period of engagement, the needle tooth at point $j^{(1)}$ engages with the cycloid gear at point $j^{(2}$. Throughout this engagement phase, the needle tooth and the cycloid gear at point j have a normal wear depth of $dh^{(1)}$ and $dh^{(2)}$, respectively, and the volumes of wear are $dV^{(1)}$ and $dV^{(2)}$, respectively. Throughout this engagement phase, the needle tooth and the cycloid gear at point j have a distance of $ds^{(1)}$and $ds^{(2)}$, respectively.

According to the Archard wear formula, for a needle tooth in a stable operational state:

$$\frac{dV^{(1)}}{ds^{(1)}} = K\frac{W}{H^{(1)}} \tag{1}$$

where K is the coefficient of wear, and W is the contact force. $H^{(1)}$ is the touch hardness, which is a constant.

The contact area at point j is dA, and the pressure at the point of contact is p. Therefore, equation (1) can be reformulated as:

$$\frac{dAdh^{(1)}}{ds^{(1)}} = K\frac{pdA}{H^{(1)}} \tag{2}$$

where the material hardness is constant, equation (2) can be simplified as follows:

$$I_h = \frac{dh^{(1)}}{ds^{(1)}} = \frac{Kp}{H^{(1)}} \tag{3}$$

where I_h is the rate of wear.

The integral form is:

$$h^{(1)} = \int KpH^{(1)}ds^{(1)}. \tag{4}$$

2.2 Contact stress

The cycloid gear engages with the needle tooth, and the contact half-width at the point of engagement can be determined as follows [11]:

$$a = 1.128\left[\frac{F_i}{b}E^*R^*\right]^{1/2} \tag{5}$$

where the equivalent modulus of elasticity

$$\frac{1}{E^*} = \frac{1-\mu_1^2}{E_1} + \frac{1-\mu_2^2}{E_2}.$$

Equivalent radius

$$R^* = \frac{R_1R_2}{R_1+R_2}.$$

The contact stress at the point of engagement is as follows.

$$P = \frac{F_i}{2ab} \tag{6}$$

where F_i is normal directional pressure of tooth profile at contact point, a is the contact half-width, b is effective tooth width of the cycloid gear, μ_1 is the Poisson's ratio of cycloidal wheel materials, μ_2 is the Poisson's ratio of needle tooth materials, E_1 is Elastic modulus of cycloidal wheel, E_2 is Elastic modulus of needle teeth, R_1 is curvature radius of the needle tooth at the contact point, R_2 is curvature radius of the cycloid gear at the contact point.

2.3 Dynamic wear coefficient

Janakiraman conducted a statistical analysis of factors such as load, speed, and lubrication characteristics during the engagement process, resulting in the wear coefficient [12]:

$$K = \frac{3.981 \times 10^{29}}{E^*}L^{1.219}G^{-7.377}S^{1.589} \tag{7}$$

where the load is:

$$L = \frac{F_i}{E^*R^*}.$$

The viscosity factor is:

$$G = \alpha_0 E^*.$$

The composite roughness is:

$$S = \frac{R_{rms}}{R^*}$$

where R^* is the equivalent curvature radius, α_o is the coefficient of viscosity, R_{rms} is the root mean square value of the tooth surface roughness, and E^* is the equivalent elastic modulus.

2.4 Amount of wear and tear

For each engagement of the cycloid gear with the needle tooth, the friction distance is determined as [13]:

$$S = 2a\lambda \tag{8}$$

where λ is the slide coefficient and a is the contact half width.

After a period of operation, the total friction distance is:

$$X = Snt\varepsilon_\alpha \tag{9}$$

where t is the work time, n is the cycloid gear speed, and ε_a is the overlap ratio of the cycloid gear.

The amount of wear at the point of engagement is as follows:

$$h_I = XI_h. \tag{10}$$

From equations (8), (9) and (10), the amount of wear is

$$h_I = 2a\lambda nt\varepsilon_\alpha I_h. \tag{11}$$

In the formula, the wear depth at the point of engagement is used to indicate wear, and the unit is m.

2.5 Calculation of the transmission error after wear

The wear amounts of the cycloid gear and the needle tooth are equated to the cumulative error in the pitch of the cycloid gear and the pitch of the needle tooth, respectively. Subsequently, the cumulative error in the circumferential direction is converted into a line of action to derive the equivalent error of the cycloid gear and needle tooth as follows [14]:

$$e_c = h_I\sin(\alpha_i - \varphi_{ci}) \tag{12}$$

$$e_p = 2h_I\sin(\alpha_i - \varphi_i) \tag{13}$$

where α_i is the angle between the line between the needle center and the contact point and the positive direction of the y-axis, φ_i is the angle between the needle tooth radius and the positive direction of the y-axis of the cycloid wheel, and φ_{ci} is the angle between the line between the needle center and the center of the cycloid gear and the positive direction of the y-axis, as depicted in Figure 2.

Excluding other error factors, the transmission error resulting from wear can be calculated using equations (11) through (13):

$$\xi_e = [h_{\mathrm{I}}(\mathrm{t})\sin(\alpha_i - \varphi_{ci}) + 2h_I(t)\sin(\alpha_i - \varphi_i)]/i_c \tag{14}$$

where i_c is the transmission ratio of the cycloid gear to the output disc.

The total transmission error of the precision planetary cycloid reducer is:

$$\xi = \xi_{in} + \xi_e \tag{15}$$

where ξ_{in} is the initial transmission error of the reducer.

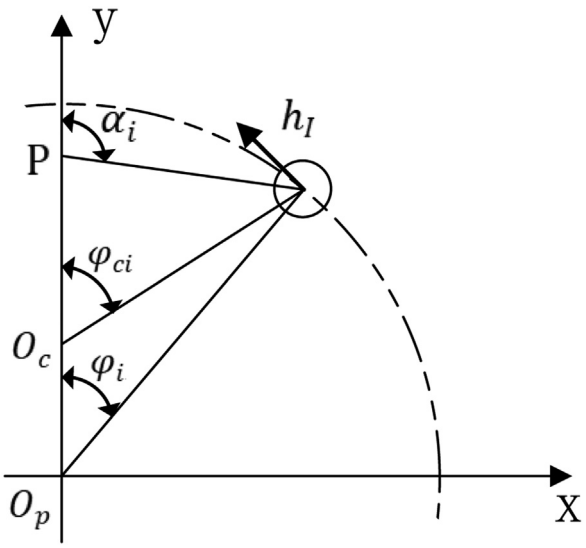

Fig. 2. Wear model of the cycloid gear and needle tooth.

3 3D simulation analysis

3.1 3D modeling

Using the precision planetary cycloid 80E reducer as a reference, we constructed distinct 3D models for various wear levels. The key parameters for the gear components of the precision planetary cycloid 80E reducer are outlined in Table 1. By applying the calculation outlined in equation (11), we determined the wear volume at various time intervals. Table 2 presents the wear volume at different time points for both the cycloid and needle gears.

Considering that wear occurs during the engagement of the cycloid gear with the needle teeth, the wear-induced changes in the cycloid gear are integrated into the tooth profile. The equation governing the tooth profile of the cycloid gear is as follows [15]:

$$\begin{aligned} x &= \left(R_p + \Delta R_p\right)\cos\left[\left(1 - i^H\right)\theta_i\right] - a\cos\left(i^H\theta_i\right) \\ &+\left(r_{rp} + \Delta r_{rp} + h_{Ic}\right)S^{-\frac{1}{2}}\left\{k_1\cos\left(i^H\theta_i\right) - \cos\left[\left(1 - i^H\right)\theta_i\right]\right\} \\ y &= \left(R_p + \Delta R_p\right)\sin\left[\left(1 - i^H\right)\theta_i\right] + a\sin\left(i^H\theta_i\right) \\ &-\left(r_{rp} + \Delta r_{rp} + h_{Ic}\right)S^{-\frac{1}{2}}\left\{k_1\sin\left(i^H\theta_i\right) + \sin\left[\left(1 - i^H\right)\theta_i\right]\right\} \end{aligned} \tag{16}$$

where the transmission ratio

$$i^H = \frac{Z_p}{Z_c}.$$

Short amplitude factor

$$k_1 = \frac{aZ_p}{R_p}$$

where X is the Cycloidal gear tooth profile equation X-coordinate, Y is the Cycloidal gear tooth profile equation Y-coordinate, h_{Ic} is wear amount of cycloid gear, R_p is radius of the needle tooth center circle, r_{rp} is needle teeth radius, a is eccentricity, θ_i is azimuth, ΔR_p is shift correction coefficient, Δr_{rp} is isometric modification coefficient, Z_p is number of needle teeth, Z_c is number of cycloidal gear teeth.

In the construction of the 3D model for the needle tooth, we begin by subtracting the wear value from its initial radius to determine the post-wear radius dimension. Subsequently, we utilize this calculated radius dimension to create the 3D model of the cycloid gear in accordance with the tooth profile equation. Figure 3 depicts the resulting 3D model of the cycloid gear. By assembling the 3D model of this component, we achieve the complete model of the precision planetary cycloid 80E reducer, as illustrated in Figure 4.

3.2 Dynamic simulation analysis

The established assembly model of the precision planetary cycloid 80E reducer was transformed into the Parasolid*. x_t format and subsequently imported into ADAMS. First, the material properties of each component are specified as follows: the input gear shaft is composed of 15CrMo material, the planetary spur gear is made of 38CrMoAl, the crankshaft and needle gear are constructed from GCr15, and the cycloid wheel is crafted from 20CrMo. Next, constraints are applied between various components: the needle gearbox and the needle gear are firmly fixed, the planetary wheel and crankshaft are also securely fixed, the output flange of the reducer is set to rotate, and the involute sun wheel is likewise configured for rotation. The angular velocity of the involute sun wheel serves as the input for the entire system, while the load torque of the output flange represents the system's output. The contact conditions between components were established as follows: rigid contact between the balance wheel and the needle tooth, contact between the crankshaft and the output flange, contact between the involute sun wheel and the planetary wheel, and contact between the crankshaft and the balance wheel. These contacts possess a rigidity of 1×10^5 N/mm, a force index of 2.2, a damping coefficient of 10 N-s/m, and a penetration depth of 0.1 mm.

In accordance with the motion characteristics of the reducer, the input speed function and load torque function for the precision planetary cycloid 80E reducer have been defined, as outlined in Table 3 [16]. The verification results for the angular velocities and reduction ratios of the key components are presented in Table 4.

Table 4 reveals that when comparing the simulation values with the theoretical values, it is evident that the virtual prototype model demonstrates a high degree of accuracy.

To further analyze the system's performance, the output shaft speeds at various stages of wear are exported in .txt format and subsequently imported into MATLAB. It is then processed using the transmission error formula to derive the corresponding transmission error curves. The

Table 1. Main parameters of gear parts of the precise planetary cycloidal 80e reducer.

Name	Numerical values	Name	Numerical values
Involute gear modulus/mm	2.6	Number of cycloid teeth	39
Number of teeth for involute sun wheels	18	Number of needle teeth	40
Number of teeth of involute planetary wheels	36	Radius of the distribution circle of the needle teeth/mm	114.5
Cycloidal pinion eccentricity/mm	2.2	Needle tooth radius/mm	5
Isometric Offer Factor/mm	0.05	Shifting distance offer factor/mm	0.05

Table 2. Wear amounts of the cycloid gear and needle gear at different times.

Working hours/h	1000	2000	3000	4000	5000	6000
Amount of wear and tear/mm	0.004732318	0.009463114	0.013549828	0.018062679	0.021986972	0.026377444

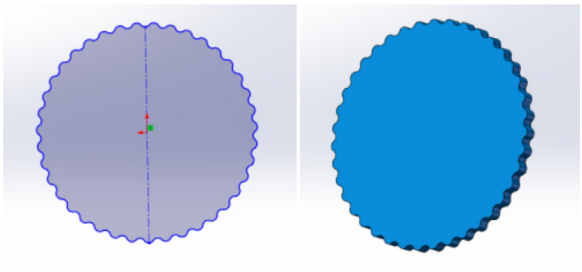

Fig. 3. Three-dimensional model of the cycloid gear.

transmission error curves for the cycloid and needle gears at different stages of wear are graphically illustrated in Figure 5.

As depicted in Figure 5 and Table 5, when the precision planetary cycloid reducer operates for 1000 h, the wear on both the cycloid gear and the needle tooth is minimal. Consequently, the clearance between the cycloid gear and the needle tooth remains small. This results in relatively minor fluctuations in the transmission error, with amplitudes ranging from −0.1684' to 0.181'. However, as the operating time increases, the clearance between the cycloid gear and the needle tooth gradually increases. This, in turn, leads to more significant fluctuations in the transmission error. For instance, after 6000 h of operation, the transmission error amplitude varies between −0.1652' and 0.4351'.

4 Transmission error theoretical calculation and simulation

In MATLAB, equation (15) is employed for calculation, resulting in the theoretical transmission error curve corresponding to the wear time of the cycloid gear and the needle tooth, as illustrated in Figure 6. Furthermore, through the simulation and calculation of the 3D model of the precision planetary cycloid reducer at various time points, the simulation-generated transmission error curve with respect to the wear time of the cycloid gear and the needle tooth was obtained, as presented in Figure 7.

From Figures 6 and 7, it can be concluded that as the working time of the RV reducer increases, the wear of the cycloidal gear and needle teeth increases. At the beginning of the transmission error, the growth trend is slower, but after 3000 hours, the growth trend of the transmission error is steeper. The speed of the increase in transmission error becomes faster, and the overall transmission accuracy begins to decrease.

5 Experimental research

To validate the accuracy of the simulation results, experimental testing was conducted on the gearbox prototype. The measuring instrument (Fig. 8) is a comprehensive performance measuring instrument for planetary cycloidal reducers. This instrument mainly includes precision mechanical systems, measurement and control systems, and measurement software, used to measure transmission errors, static backlash, dynamic backlash, etc. of reducers. The input end of the planetary cycloidal reducer is driven by an input motor, and the output end is mainly loaded by a load motor on the output shaft of the reducer, and the size of the load is adjusted by the computer controlled motor. A high-precision circular grating was used to detect the rotation angle of the input and output of the system, and a dual channel torque sensor was used to detect the torque of the system. To comprehensively investigate the evolution of the transmission error in a planetary cycloid reducer, a degradation test was conducted using a constant stress loading mode. The rated load was set at 1.5 times the constant stress loading,

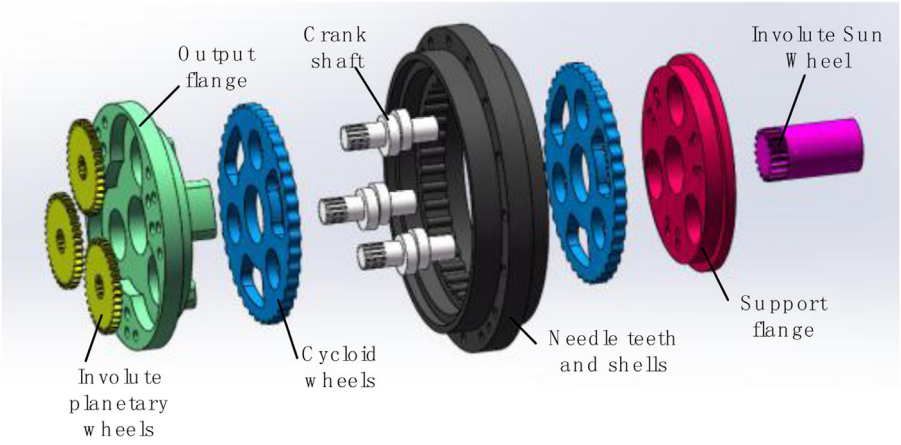

Fig. 4. Precise planetary cycloidal 80e reducer model.

Table 3. Precise planetary cycloidal 80e reducer input speed function and load torque function.

Projects	Function expressions
Sun wheel input speed/((°)/s)	Step (time ,0,0,0.01,7290d)
Output disc load tor que/(N mm)	Step (time ,0,0,0.01,−784000)

Table 4. Verification of the angular velocity and reduction ratio of the key parts.

Projects	Theoretical value	Simulation values	Relative error/%
Angular velocity of the solar wheel/((°)/s)	7290	7290	0
Angular speed of the planetary wheel /((°)/s)	3645	3708.8	1.8
Output disc angular speed /((°)/s)	90	93.4	3.8
Reduction ratio of the whole machine	81	78.1	3.6

and measurements of transmission accuracy were taken at regular intervals during the test. A representative forward transmission error curve is presented in Figure 9.

An analysis of the error curve in Figure 9 clearly reveals that after a certain initial period, when subjected to a load 1.5 times its rated capacity, the transmission error of the prototype experiences only a modest increase. However, with prolonged operation, the transmission error of the prototype exhibits a more pronounced increase, signifying a more significant decrease in transmission accuracy.

To comprehensively analyze the evolution of the transmission error in the precision planetary cycloid gearbox prototype, the results of the transmission error obtained from all tests conducted during the gearbox degradation test were plotted on a two-dimensional diagram. This overview is presented in Figure 10, which provides a holistic perspective on the transmission error change process.

Figure 10 reveals that the transmission error initially exhibited a slight increase at a low value during the initial test. However, in the subsequent tests, the rate of increase in the transmission error was notably greater. The measured transmission errors further demonstrated that these values continued to rise as the prototype's running time increased.

6 Conclusions

In this investigation, predicated upon the motion of the cycloid pinwheel and needle tooth during the meshing procedure, the wear magnitude of these components is computed in accordance with the Arcadian wear model and the error theory. Additionally, a functional correlation between the wear duration of these elements and the transmission error of the overall apparatus is derived. Subsequently, the wear model is simulated and scrutinized utilizing ADAMS software. Ultimately, the inquiry is substantiated through empirical experimentation.

The outcomes demonstrate that the theoretical transmission error curve is fundamentally congruent with the simulated transmission error curve. The fluctuation in the transmission error remains nominal as the cycloid needle teeth initiate wear and gradually intensify as the gear teeth wear down. This manifestation is encapsulated

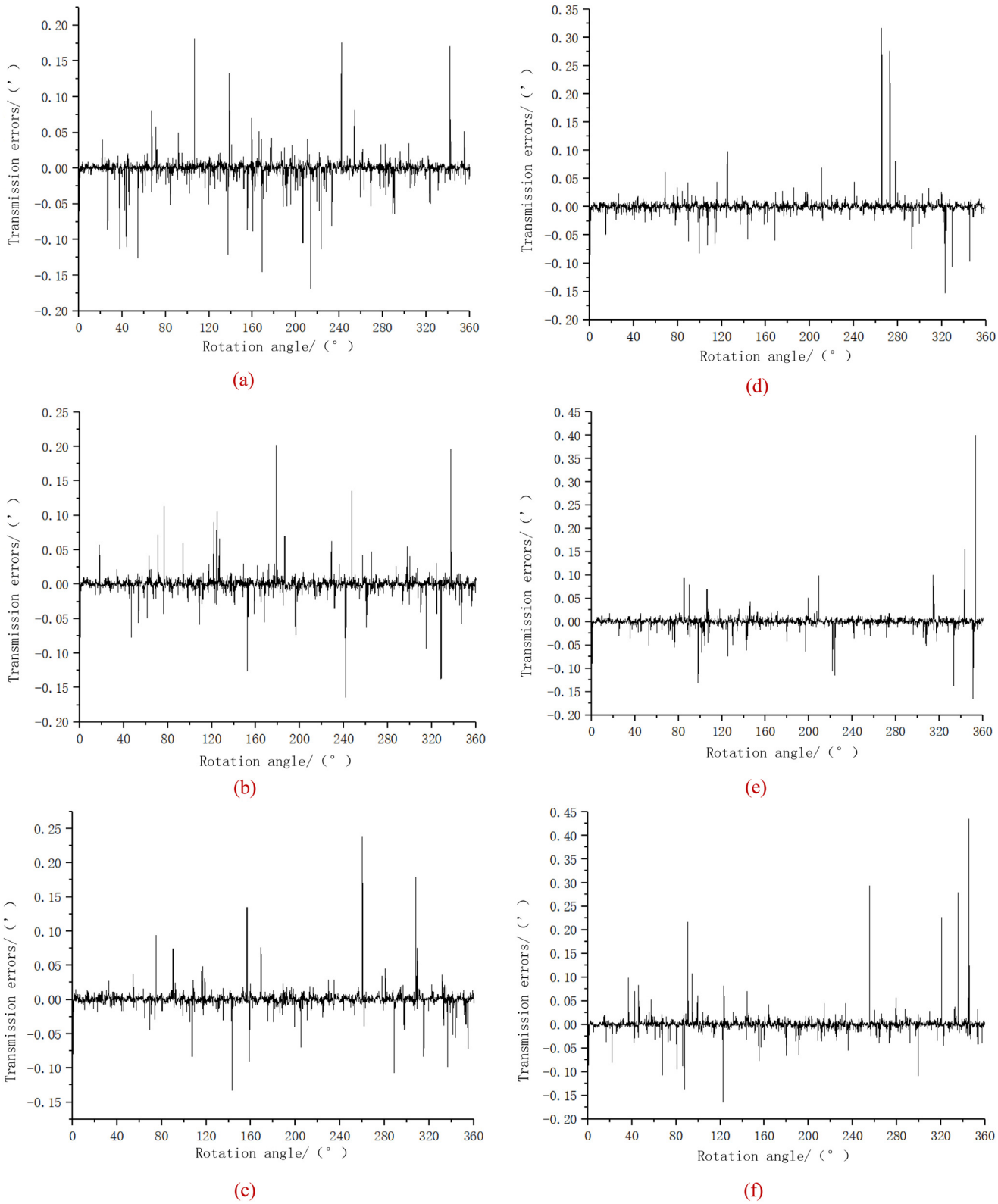

Fig. 5. Transmission error curves after wearing the cycloid gear and needle tooth. (a) Wear 1000 h transmission error curve. (b) Wear 2000 h transmission error curve. (c) Wear 3000 h transmission error curve. (d) Wear 4000 h transmission error curve. (e) Wear 5000 h transmission error curve. (f) Wear 6000 h transmission error curve.

Table 5. Amplitude range of transmission error under different wear times.

Wear time/h	1000	2000	3000	4000	5000	6000
Maximum value/‘	0.1810	0.2016	0.2389	0.3164	0.4006	0.4351
minimum value/’	−0.1684	−0.1639	−0.1326	−0.1529	−0.1652	−0.1652

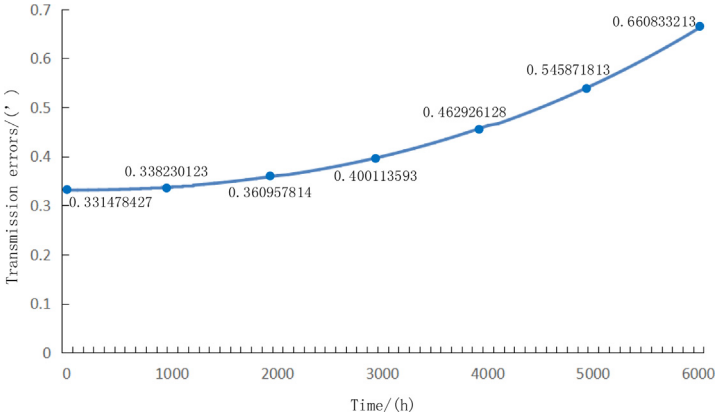

Fig. 6. Theoretical curve of transmission error as a function of wear time for the cycloid and needle teeth.

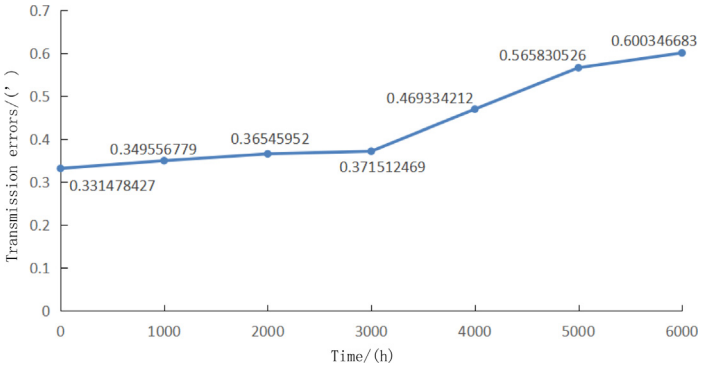

Fig. 7. Simulation curve of transmission error with wear time for the cycloid and needle teeth.

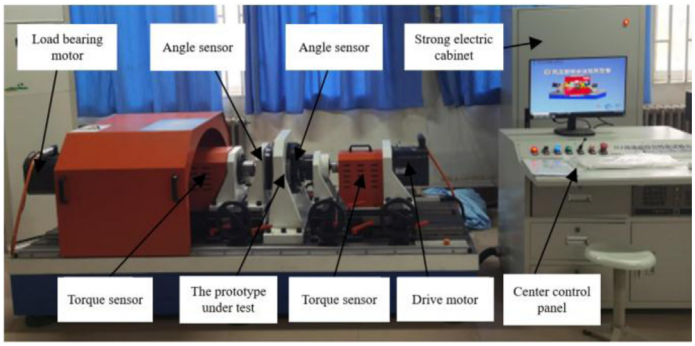

Fig. 8. The measuring instrument.

in the cycloid gear profile equation, signifying an increase in the isometric trimming value. An increase in the isometric trimming value precipitates augmented transmission error in the gearbox, consequently reducing its precision. The deductions drawn from the experimental inquiry further affirm the fidelity of the simulation outcomes. This approach offers a pivotal point of reference for delving into the process of accuracy degradation in planetary cycloidal gearboxes and for enhancing their operational lifespan.

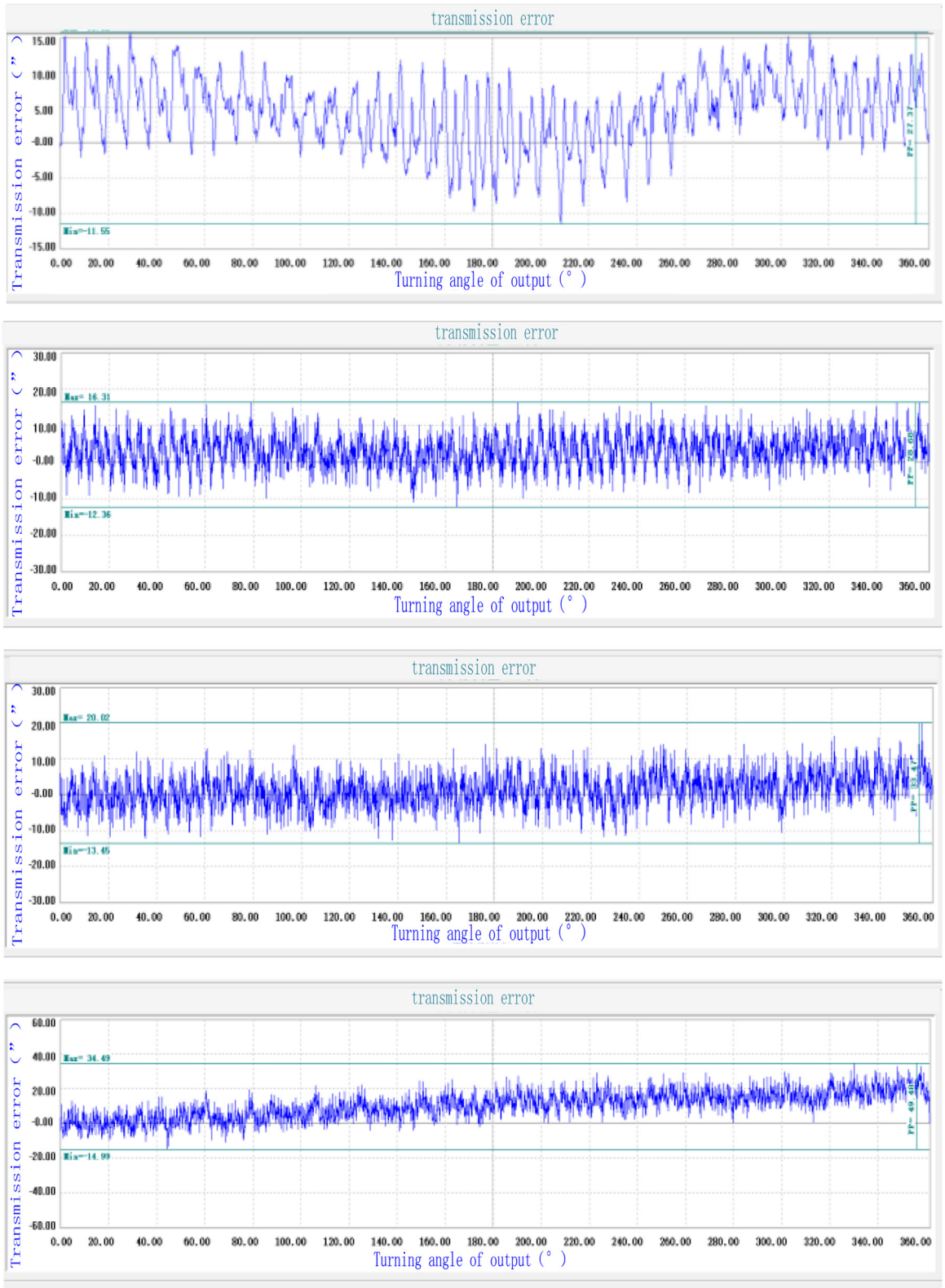

Fig. 9. Precision planetary cycloidal gearbox transmission errors for different operation times.

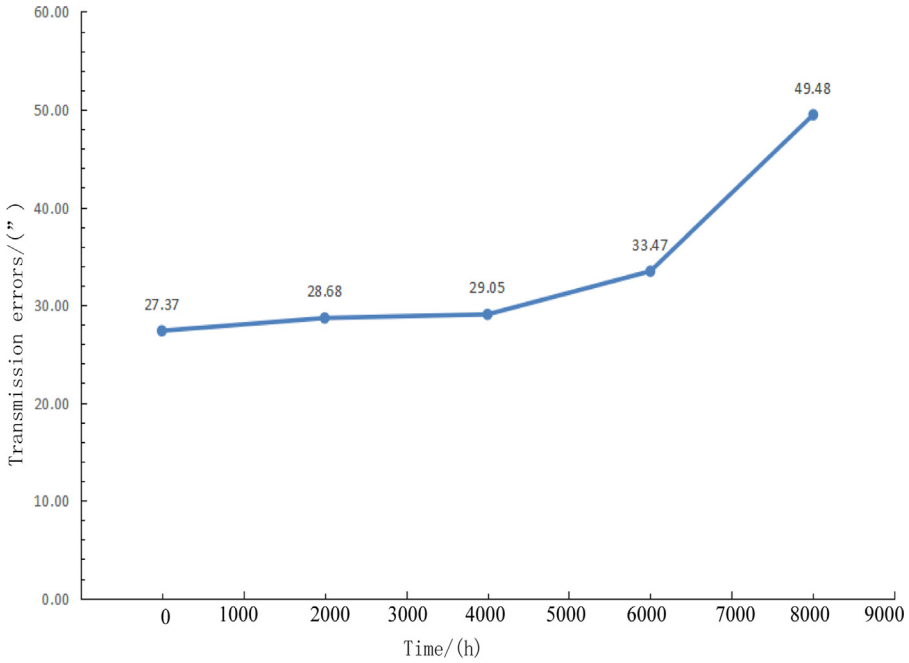

Fig. 10. Transmission error curve with the running time of the prototype.

Acknowledgments

The work was supported by the National Natural Science Foundation of China (No. 52075561).

Funding

Funding for this paper is supported by the National Natural Science Foundation of China 2020 (Project number: E0502).

Conflict of Interest

No conflict of interest exists in the submission of this manuscript, and manuscript is approved by all authors for publication.

Data availability

The data in this paper are obtained by simulation analysis.

Author contribution statement

Author 1 (First Author): Conceptualization, Formal Analysis, Project Administration, Funding Acquisition, Writing-Review & Editing; **Author 2:** Investigation, Writing-Original Draft, Software; **Author 3:** Visualization, Investigation, Data Curation; **Author 4:** Formal Analysis, Validation; **Author 5:** Supervision; **Author 6:** Resources; **Author 7:** Methodology.

References

1. Y. Zheng, H.-l. Wang, J.-x. Su, Transmission error analysis of RV reducer and simulation based on ADAMS, Mach. Tool Hydraulics **47**, 133–138 (2019) in Chinese)
2. B.-s. Pan, C.-k. Lin, Y.-y. Xiang et al., Transmission time-variant reliability analysis and optimization design of planetary reducers considering gear wear, Comput. Integr. Manufactur. Syst. **28**, 745–757 (2022) (in Chinese)
3. K. Zeng, A Electric-Enclosed Test Rig for Worm Gear Full-Life Wear [D]. Chongqing University of Posts and Telecommunications, Chongqing (2021) (in Chinese)
4. J.-y. Li, J.-x. Wang, K.-j. Fan et al., Accelerated life model for harmonic drive under adhesive wear, Tribology **36**, 297–303 (2016) (in Chinese)
5. L. Wang, The Reliability Analysis of Harmonic Reducer Based on The Wear Mechanism [D]. University of Electronic Science and Technology of China, Chengdu (2020) (in Chinese)
6. C.-k. Lin, Transmission accuracy reliability analysis and optimization of planetary reducers considering gear wear [D]. Zhejiang University of Technology, Hangzhou (2020) (in Chinese)
7. S.-r. Wang, Y.-t. Yan, J.-y. Ding, Experimental study on mesh-wear of involute spur gears, J. Northeastern Univ. (Natural Science) **25**, 146–149 (2004) (in Chinese)
8. W.-c. Song, Numerical calculation of helical gear wear in high-precision synchronous transmission [D]. Harbin Institute of Technology, Harbin (2011) (in Chinese)
9. J.-r. Cao, Y. Feng, B.-c. Lu et al., Wear trend prediction of crane gearbox based on OSVR method with combined kernel functions, China Mech. Eng. **26**, 641–646 (2015) (in Chinese)
10. J.F. Archard, Contact and rubbing of flat surfaces, J. Appl. Phys. **24**, 981–988 (1953)
11. J.-x. Su, C. Li, Numerical calculation and analysis of cycloidal gear wear amount of RV reducer, Mech. Transmiss. **45**, 41–45+57 (2021) (in Chinese)
12. V. Janakiraman, An investigation of the impact of contact parameters on the wear coefficient [D]. The Ohio State University, Columbus (2013)
13. G.-y. Lin, D. Feng, X.-y. Zheng et al., Analysis of the impact of extrusion times on die wear based on Archard theory, J. Central South Univ. (Natural Science Edition) **40**, 1245–1251 (2009) (in Chinese)
14. Y. Yan, Research on drive accuracy and inherent characteristic of RV reducer [D]. Xiangtan University, Xiangtan (2014) (in Chinese)

15. H. Wang, Research on accuracy characteristics of RV reducer for robot [D]. Engineering Beijing University of Technology, Beijing (2019) (in Chinese)
16. Y.-c. Li, S. Yuan, Z.-j. Fan, Dynamic simulation study of 3k planetary reducer with clearance, Mech. Des. Manufact. **12**, 9–13 (2021) (in Chinese)

Cite this article as: Hang Xu, Chenzhou Wei, Wei Gui, Shufeng Yang, Yuanchun He, Guiping Xie, Yaoting Wu, Investigation of the impact of cycloidal gear pin tooth wear on transmission error in precision planetary cycloidal reducers, Int. J. Metrol. Qual. Eng. **15**, 9 (2024)